NASA
Technical Memorandum 81570

AVRADCOM
Technical Report 80-C-15

The Role of Oxidation in the Fretting Wear Process

Robert C. Bill
Propulsion Laboratory
AVRADCOM Research and Technology Laboratories
Lewis Research Center

Prepared for the
International Conference on Wear of Materials
cosponsored by the American Society of Mechanical Engineers
and the Japan Society of Mechanical Engineers
San Francisco, California, March 30-April 1, 1981

NASA

US ARMY AVRADCOM

THE ROLE OF OXIDATION IN THE FRETTING WEAR PROCESS

by Robert C. Bill

National Aeronautics and Space Administration
Lewis Research Center
Cleveland, Ohio 44135

E-538

ABSTRACT

Fretting experiments were conducted on titanium, a series of Ni-Cr-Al alloys and on some high temperature turbine alloys at room temperature and at elevated temperatures in air and in various inert environments. It was found that, depending on temperature and environment, the fretting behavior of the materials examined could be classified according to four general types of behavior. Briefly, these types of behavior were: (1) the complete absence of oxidation, as in inert environments, generally leading to low rates of fretting wear but high fretting friction; (2) gradual attrition of surface oxide with each fretting stroke, found in these experiments to operate in concert with other dominating mechanisms; (3) rapid oxidation at surface fatigue damage sites, resulting in undermining and rapid disintegration of the load bearing surface; and (4) the formation of coherent, protective oxide film, resulting in low rates of fretting wear. An analytical model predicting conditions favorable to the fourth type of behavior was outlined. Classification of the fretting behavior of the materials examined into the four types described above was shown to be consistent with published oxidation behavior and kinetics.

NOMENCLATURE

B	fretting stroke amplitude (m)
B_e	dislocation core energy $\left(\sim 6 \times 10^{-5} \frac{erg}{cm}\right)$
b	Burger's vector ($\sim 2.5 \times 10^{-8}$ cm)
C_1	fretting wear rate coefficient ($cm/sec^{1/2}$)
C_2	oxidation rate coefficient (cm^2/sec)
f	fretting frequency (Hz)
G	shear modulus (MN/m^2)
K_{ox}	wear coefficient of oxide (dimensionless)
K_p	parabolic oxidation rate ($cm/sec^{1/2}$)
L	normal load (N)
P_m	hardness of metal (MN/m^2)
R	radius of curvature of contact surface (cm)
x	instantaneous oxide film thickness (cm)
$\dot{x}$	rate of growth of oxide film (cm/sec)
ν	Poisson's ratio
θ	tilt boundary angle (deg)
γ_w	tilt boundary wall energy (erg/cm^2)

INTRODUCTION AND BACKGROUND

The importance of oxidation to the fretting process has long been recognized and is implicit in the often used expression "fretting corrosion." There is considerable published data illustrating the significance of oxidation, oxide debris and the formation of oxide films in the fretting process.[1-5] By way of classic example, let us compare room temperature fretting in air with fretting in N_2. Greatly increased adhesion between fretting metal pairs was reported by Waterhouse[6] when fretting was conducted in N_2 rather than air, generally attributed to increased metal-to-metal contact in N_2. Despite the increased adhesion, fretting wear rates in N_2 were observed by Feng and Uhlig[4] and others[7,8] to be at least an order of magnitude lower than those determined from fretting experiments in air.

When a metal undergoes fretting at elevated temperatures in air, the surface oxides formed become quite significant to the fretting process. Such things as adherence of the oxide to the substrate, mechanical properties of the oxide, thickness, rate of growth, composition and structure of the oxide film probably determine whether the film will inhibit or accelerate fretting wear. Unfortunately, little specific information is available on the adherence and mechanical properties of oxide films. However, the composition and structure of oxide films have received much attention.

The particular oxides that form generally depend on temperature and bulk composition of the alloy. For example, in the extensively studied Ni-Cr system, exposure to oxidation at 700° C results in an equilibrium oxide consisting of $NiCr_2O_4$ particles in a NiO matrix for alloys of less than 10 atomic percent Cr. For alloys of more than 10 atomic percent Cr, a continuous Cr_2O_3 film forms.[9,10] Additions of Al to the Ni-Cr system result in complex layered oxides according to Giggins and Pettit,[11] and Stott, et al.[12] Even in elemental metal systems, oxide film formation is often complex. Above 570° C, iron

for example, shows a layered oxide scale structure consisting of FeO adjacent to the Fe substrate, an intermediate layer of Fe_3O_4, and Fe_2O_3 adjacent to the oxidizing environment (ref. 9, p. 128). Below 800° C, the oxide that forms on Ti is entirely TiO_2, while at higher temperatures a layered morphology is observed.(13)

Extensive oxide film growth studies have been performed on a number of elemental metals and alloy systems. Growth kinetics generally follow one of four rate laws: (1) logarithmic, (2) parabolic, (3) cubic, and (4) linear. Logarithmic oxidation rates usually apply at low temperatures (up to 200° to 300° C), and the rate governing physical mechanisms are variously described as adsorption, chemisorption, and electric field induced ionic transport.(14) At higher temperatures, ionic dissolution rates and diffusion through comparatively thick oxide layers lead to parabolic or cubic oxidation kinetics, in which the oxide film thickness is proportional to exposure time to the 1/2 power (parabolic) or 1/3 power (cubic). With further increases in temperature, debonding of the oxide film, probably due to defect coalescence at the oxide/metal interface, sometimes leads to linear oxidation rates.

For a given metal, temperature determines which oxidation rate law predominates, and the associated rate constant. Correlation between fretting studies and oxidation rates have been shown.(2,3,15,16) The conclusion drawn from these studies is that for the oxide film to effectively reduce fretting wear, a critical film thickness must be maintained in the fretting contact area. As more rapid growth kinetics predominate at elevated temperatures, fretting resistance generally increases, provided the oxide film remains adherent to the substrate.

In this paper, the effect of temperature on the fretting wear of Ti, a series of Ni-Cr-Al alloys, and a series of high temperature turbine alloys is studied. Titanium and the Ni-Cr-Al alloy series were of interest because of the availability of oxidation data for these metals. Fretting of the high temperature turbine alloys was of practical interest in the space shuttle liquid hydrogen turbopump, and these alloys were subjected to fretting in air and in argon. The object of bringing these data together in this paper is to develop a better understanding of the interaction between the fretting process and oxidation.

APPARATUS AND PROCEDURE

A schematic diagram of the fretting rig is shown in figure 1. Linear oscillatory motion is provided by an electromagnetically driven vibrator with the frequency controlled by a variable oscillator. The amplitude of the motion was controlled to 70±5 μm in most cases, and the frequency employed was usually 80 Hz. The normal load, applied by placing precision weights on a pan hung from the load arm, was 1.47 N, except for a series of load variation experiments performed on titanium.

The fretting specimens include an upper, stationary 4.76 mm radius hemispherical tip in contact with a lower flat which is driven by the vibrator. Before assembly into the rig, the flat specimens were lapped, mechanically polished with 0.05 μm alumina polishing compound, then rinsed in pure ethanol. The hemispherical tips, ground to a 0.1 μm finish, were scrubbed with 0.05 μm alumina, then rinsed. In all cases, except for those involving MAR M-246, the upper and lower specimens were of the same composition.

During high temperature experiments, the specimen and grip assemblies were surrounded by a 310 stainless steel susceptor which was heated by an induction coil. The temperature was monitored by a thermocouple probe mounted in the lower grip.

A dry air environment was provided by flowing air through an absorption drier, then into the test chamber. In this way, moisture content was kept in the range of 10 to 100 ppm. Alternately, a selected inert gas (nitrogen or argon) was used. A one hour purge time was employed in all cases prior to starting fretting in the selected environment.

Following each experiment the fretting scar on the flat surface was photographed to record the size and features of the wear scar and the debris accumulation around the scar. The loose debris was then rinsed off with pure ethanol and a light section microscope, described in reference 17, was used to measure the wear volume on the flat specimen. Specimens that were examined in the scanning electron microscope (SEM) were ultrasonically cleaned before viewing to remove as much debris still adhering to the wear scar as possible.

MATERIALS

The materials studied in this investigation include high purity titanium, a series of Ni-Cr-Al alloys, and a series of high temperature gas turbine alloys.

The high purity titanium was 99.8% pure, the chief impurities being carbon (150 ppm), silicon (150 ppm), and oxygen (350 ppm). In the as machined condition the hardness was Rockwell B-74. After exposure to 650° C for one hour in air, the hardness was Rockwell B-69. Further exposure to 650° C in air resulted in no further reduction in hardness.

Four Ni-Cr-Al alloys were studied, and their compositions were, by weight percent: Ni-10% Cr-2% Al; Ni-10% Cr-5% Al; Ni-20% Cr-2% Al; Ni-20% Cr-5% Al. The alloys were prepared from elemental metals of 99.9 + percent purity, vacuum melted in a zirconia crucible and cast in graphite molds. The as cast Rockwell B hardnesses of the Ni-Cr-Al alloys were as follows: Ni-10% Cr-2% Al, 61 R_B; Ni-10% Cr-5% Al, 98 R_B; Ni-20% Cr-2% Al, 80 R_B; Ni-20% Cr-5% Al, 102 R_B.

The high temperature turbine alloys studied included MAR M-246, a turbine blade alloy; Haynes-188, a candidate blade vibration damper alloy; and A-286, another blade vibration damper candidate. The nominal compositions (wt. %) of these alloys are as follows: MAR M-246, Ni-10% Co-9% Cr-10% W-5.5% Al-2.5% Mo-1.5% Ti-1% Fe-0.15% C-0.1% Mn; Haynes 188, Co-22% Ni-22% Cr-14% W-3% Fe-0.1% C-0.04% La; and A-286, Fe-26% Ni-15% Cr-2.15% Ti-1.4% Mn-1.25% Mo-0.2% Al-0.4% Si-0.05% C-0.03% V.

RESULTS

General Effects of Oxidation on Fretting

Fretting wear result for titanium, typical of those for a wide range of materials in air and N_2 at room temperature, are shown in figure 2. Initially, the wear rate was fairly high, reflecting a run-in period extending over 10^2 to 10^3 cycles in both air and N_2. Following run-in, a period of very low rate fretting wear is seen. During this period, micro-spall pits first appear as shown in the micrograph of figure 3. The appearance of micro-spall pits

is taken to indicate a transition from adhesive and plastic flow dominated wear mechanisms to a more gradual fatigue disruption of the fretting surface. After 10^4 to 10^5 fretting cycles, significant differences in fretting wear rate and appearance of the fretting surfaces begin to appear, depending on whether fretting was conducted in air or N_2. When fretting was conducted in air, accelerated fretting wear was observed, and the micro-spall pit edges began to exhibit a "leafy" or fringed appearance. This fringed appearance is believed to indicate accelerated disintegration of the pit edges through a combination of fatigue and oxidation. In contrast, the pit edges after 10^5 fretting cycles in N_2 still appear quite sharp and well defined, as shown in figure 3.

Further evidence of the effect of oxidation on fretting wear and friction of several high temperature alloys is shown in figure 4. Results of experiments conducted at room temperature and elevated temperatures in both air and dry argon on some high temperature turbine alloys are presented. At room temperature, fretting wear in air was two-to-three times that in dry argon. Wear scar surfaces, resulting from fretting in dry air and dry argon are shown in figure 5. Spall pits and accumulated debris are present on the surfaces fretted in air, while the surfaces fretted in argon show micro-regions of intense plastic deformation and smearing, but little pitting and no debris whatever.

At elevated temperatures, more wear was observed in dry argon than in dry air, as may be seen in figure 4. Friction at elevated temperatures was also higher in dry argon than in dry air, although it was considerably lower than at room temperature.

Fretted surfaces resulting from experiments in dry argon and dry air at high temperatures are shown in figure 6. Pitting is apparent after fretting in dry argon, with large regions of direct adhesive transfer of material from one surface to another. In comparison, the surface resulting from fretting in air is fairly smooth and featureless.

Fretting of Ni-Cr-Al Alloys

The results of fretting wear experiments performed on a series of four Ni-Cr-Al alloys are summarized in figure 7. For all alloys studied, the wear volume at 540° C was about an order of magnitude less than that observed at room temperature. Also, wear of the 20% Cr alloys was consistently less than that of the 10% Cr alloys at room temperature and at 540° C. At 650° C the 20% Cr alloys showed significantly more wear than at 540° C, and at 816° C build-ups of material like those shown in figure 8 were observed on the fretted surfaces. On the other hand, the 10% Cr alloys showed little increase in wear as the temperature was increased from 540° to 650° C. No build-ups of material were observed on the fretted surfaces of 10% Cr alloys at 816° C. Instead, material removal occurred, and micro-spall pits like those shown in figure 9 were seen.

X-ray dispersion analyses of sectioned 20% Cr specimens showed strong Cr and Al peak height gradients beneath the fretted surface, as summarized in figure 10. The Cr relative peak height near the surface is about 50% higher than that representing bulk concentration, while aluminum relative peak heights are 4 to 5 times those of the bulk. The apparent composition profiles for the 20% Cr alloys were about the same directly under the fretting wear scar and away from the fretted area.

Though no sectional analyses were conducted, X-ray dispersion analysis studies of fretted and unfretted surfaces on Ni-10 Cr-5 Al samples do show significant differences which are indicated in figure 11. The Al peak height within the fretted area is 2 to 3 times the peak height elsewhere on the specimen surface. Although X-ray dispersion analysis is not strictly a surface examination technique, the peak heights result from surface region concentrations superimposed on subsurface bulk concentrations to a depth of 3 or 4 μm. Most likely, the only differences between material examined within and outside the fretting scar are in the surface region compositions. Therefore, the difference in Al peak height within and outside the fretting scar for the Ni-10 Cr-5 Al alloy probably indicates a real change in Al concentration on the fretting wear scar surface. No significant difference between the Al concentration within and outside the fretting scar was observed on the Ni-20 Cr-5 Al specimen.

Fretting of Titanium

The fretting wear volume of titanium is shown in figure 12 as a function of temperature. Micrographs, representative of the fretted surface at various temperatures are also shown. There are two distinct regions in the fretting wear volume versus temperature curve. Initially, wear increases with temperature up to 450° C. Somewhere between 450° and 540° C, the wear volume goes through a maximum. At temperatures of 540° C and above, a trend of decreasing wear volume with increasing temperature is observed.

Microscopic examination of the wear surfaces (fig. 12) shows distinctly different features below and above the temperature range in which maximum wear is observed. At temperatures below 450° C, micro-spall pits are present, accompanied by loose oxidized debris. Above 540° C the fretted surface is quite smooth with no pitting and no debris in evidence; cracks are sometimes present, generally oriented perpendicular to the direction of fretting motion. Apparently, the fretting contact stresses were completely supported by a continuous, thick oxide film above 540° C. Below 450° C the film was not sufficiently thick to resist disruption under fretting conditions.

In figure 13, fretting wear volume is shown as a function of number of fretting cycles for four values of contact load at 650° C. At loads of 0.29 N and 0.74 N, wear volume was more or less a single slope linear function of number of cycles. Fretted surfaces were almost featureless. At 1.47 N, the standard load condition, a rather pronounced discontinuity in wear rate between 10^5 and $3x10^5$ cycles is observed. Though no direct microscopic evidence was found, it is believed that initially high contact stresses lead to oxide film disruption early in the fretting exposure; the oxide film however, was self-repairing under these conditions and resisted further disruption. The only surface distress seen after $3x10^5$ cycle was the presence of cracks in the oxide film, noted earlier. When the load was increased to 2.94 N, the wear rate remained very high up to $3x10^5$ cycles, and pitting was observed on the fretted surface. Evidently, under this high load condition, oxide film disruption continued out to $3x10^5$ cycles.

DISCUSSION

General Types of Fretting Behavior

The preceding results suggest that for the materials evaluated, fretting wear proceeds by distinctly different mechanisms depending on temperature and environment. In general, one can identify four distinct types of fretting behavior with respect to the role played by oxidation. The four types are shown schematically in figure 14, and a summary of how the materials studied in this investigation behaved within the framework of these four types is included in table I.

First, there is the behavior resulting from fretting between metals in an inert atmosphere or between noble metals, oxidation being precluded in both cases. Metal-to-metal adhesive contact predominates, but unlike the results generally seen in unidirectional sliding experiments, fretting wear rates in inert environment or between noble metals are much lower than those observed in situations in which oxidation may occur. Apparently, under fretting conditions in which oxidation cannot occur, either strain hardening strengthens the contact surfaces preventing formation of wear particles, or the sliding distance is so small that many particles that do form readhere with no net material loss in evidence. The micrographs of figure 3 tend to support the former.

The second type of fretting behavior shown in figure 14, originally proposed by Uhlig,[18] shows material removal as occurring through the cyclic removal of an oxide film that forms on the contact surface during the interval between fretting strokes. This model of gradual attritive wear was proposed to account for Feng and Uhlig's observed inverse proportionality between fretting wear rate and fretting frequency. Supposedly, at low frequencies, a thicker oxide film can form and be removed during each fretting stroke than at high frequencies. In view of observed extensive micro-pitting, as seen in figure 3 and elsewhere, it appears unlikely to the author that this second type of fretting behavior alone accounts for the fretting process. Rather, it might act in parallel with the third type of behavior.

According to the third type of fretting behavior, fretting wear takes place through a surface fatigue process, resulting in the formation of microspall pits within the contact area. Oxidation can enter into the fretting process in two ways. On the load bearing portions of the contact area, the attritive process proposed by Uhlig might take place. Meanwhile, at the edges of the spall pits where heavily fatigued metal is exposed to the environment, oxygen may quickly diffuse into the metal promoting sub-surface oxidation and rapid laminar crack growth rates undermining the load bearing contact area. Oxygen diffusion would be aided by the high dislocation density concentrated in cell walls, typical of fatigue damage in metals. Also, crack propagation itself would be made easier by the presence of the cell walls, so suggested by the following calculation. Considering a simple tilt boundary, the expression for cell wall energy is[19]

$$\gamma_w = \frac{Gb}{4\pi(1-\nu)}\,\theta(A - \ln\theta) \qquad (1)$$

where

$$A = \frac{4\pi(1-\nu)B_e}{Gb^2}$$

For the case of $\theta = 0.1$ rad, and using copper as an example, γ_w turns out to be about 500 ergs/cm^2, a number in the same order of magnitude as the crack surface energy. The leafy appearance and layered morphology around the spall pit edges certainly suggest accelerated, nonhomogeneous deterioration of sub-surface material.

Finally, the fourth type of fretting behavior includes situations in which the oxide film remains intact and adherent to the metal substrate under fretting conditions. All wear that takes place occurs directly to the oxide film itself, with direct metal-to-metal contact never taking place. During fretting the oxide film remains sufficiently thick to support the contact load. Fretting of titanium at temperatures above 540° C in this study, and the high temperature fretting of Ni-10 Cr-5 Al alloy correspond to this type of behavior.

High Temperature Fretting of Titanium

The experiments performed on titanium support the idea that a critical oxide film thickness is required to support a given load or contact stress. Above 540° C oxidation kinetics of titanium undergo a transition from rather slow logarithmic oxidation to rapid parabolic kinetics,[9] enabling the oxide film thickness to effectively support the contact stresses. Similar arguments were put forth by Hurricks[3] to account for reduced fretting of mild steel at elevated temperatures, as noted in the Introduction. Quinn[20] proposed a critical oxide film thickness which, once reached under sliding conditions, led to loss of the oxide film and formation of a wear particle. In a later paper[21] Quinn suggested that the critical oxide film thickness is proportional to the contact load, a position consistent with the titanium results reported herein.

In an earlier treatment of the high temperature fretting results on titanium,[22] a model predicting instantaneous film thickness under fretting conditions was developed. In essence, the model coupled contact geometry parameters illustrated in figure 15(a) with assumed parabolic oxidation kinetics to give the following equation describing instantaneous film thickness and growth rates:

$$\dot{x} = \frac{C_2}{x - C_1 t^{1/2}} \qquad (2)$$

where

$$C_1 = \left(\frac{K_{ox} L f B}{3.2\, P_m R}\right)^{1/2}$$

and

$$C_2 = \frac{K_p^2}{2}$$

Equation (2) was solved numerically, and values of x were obtained as a function of time for cases representing high, intermediate, and low normal loads, determined by the value of C_1. The results are shown in figure 15(b). The values chosen for C_1 were based on wear measurements made early in the 1.47-newton normal load series (before the transition to high wear). The value for the 1.47-newton case was doubled to simulate the high normal load, and halved to simulate the low normal load. The initial

film thickness, before fretting, was on the order of 1 micrometer. Keep in mind that these results apply only so long as the oxide film remains intact, that is, fretting proceeds as under the fourth category. The significant point is that equation (2) predicts that the theoretical film thickness passes through a minimum value early in the fretting exposure under a high normal load, and no significant thinning is observed for the light load situation. Once disruption of the thinned oxide film occurs, equation (2) no longer describes the relation between oxide film growth and wear. The wear rate becomes much higher and the oxide film becomes very irregular and discontinuous.

The results may be generalized to other contact geometries. For conforming, or flat geometry cases, a uniform average rate of surface recession due to wear is predicted as long as the oxide film is not ruptured. Film thinning will continue to the point at which, according to parabolic growth kinetics, the oxide film growth rate can keep pace with wear. A steady-state film thickness is predicted. Film penetration may occur, leading to a transition to high wear, if the steady-state film thickness is insufficient to support the contact load.

High Temperature Fretting of Ni-Cr-Al Alloys

The Ni-Cr-Al alloys exhibited a mixed behavior with respect to fretting mechanisms, as indicated in table I. Differences in fretting behavior at 816° C in these alloys may be attributed to differences in the oxide layers present on the alloys prior to the onset of fretting and during fretting.

Besides the X-ray energy dispersion analyses reported herein, oxidation studies by Giggins and Pettit,[11] and Stott, et al.[12] have classified alloy compositions according to surface oxides formed at 1000° C. The results of the oxidation studies show interesting correlations with the present results at 816° C. Both of the oxidation studies cited above predicted protective Al_2O_3 films on alloys of approximately Ni-10% Cr-5% Al composition, a good situation from the standpoint of oxidation resistance. Ni-10% Cr-5% Al was the most fretting resistant alloy of the Ni-Cr-Al alloy series. The Ni-Cr-Al alloy that underwent the most severe fretting at 816° C, namely Ni-10% Cr-2% Al, roughly corresponded to compositions predicted by Stott, et al. to form a duplex Cr_2O_3 (outer) - Al_2O_3 (inner) oxide with some internal oxidation. Pettit and Giggins show this composition as borderline between being a protective Al_2O_3 former and a complex, layered oxide former with internal oxidation at 1000° C. The Ni-20% Cr-2% Al alloy, which exhibited rather large build-ups of oxidized material in the fretted area, corresponds to compositions predicted in both oxidation studies cited to form a duplex Cr_2O_3-Al_2O_3 oxide at 1000° C. Perhaps, this duplex oxide is not self repairing at 816° C, thereby, leading to localized rapid substrate oxidation at locations where the film is disrupted by fretting action. Ni-20% Cr-5% Al alloy reportedly forms a uniform Al_2O_3 film at 1000° C, but according to reference 11, the composition is quite close to the boundary between duplex film formers and uniform Al_2O_3 formers. Again, as with the Ni-20% Cr-2% Al alloy, the oxide film is perhaps vulnerable to disruption under fretting conditions, and a protective Al_2O_3 film is not readily formed at damage sites. Thus, the potential of an alloy to form a protective (from the standpoint of oxidation) Al_2O_3 film in situ also appears to provide the alloy with high temperature fretting resistance. This is consistent with oxidative wear since the Al_2O_3 film tends to grow more slowly than the various duplex oxide films, thereby requiring longer exposure times to reach a critical thickness.

CONCLUDING REMARKS

The principal points supported by the data in this paper and developed in the Discussion include the following:

1. Four types of fretting behavior, classified according to the role played by oxidation, were identified. They include: (a) completely nonprotective or noninteractive, as for the case of fretting in an inert environment or between noble metals, (b) sequential stripping away of a thin surface oxide film with each fretting cycle, (c) interaction between oxidation and surface fatigue, promoting rapid, nonhomogeneous oxidation at fatigue damage sites, and (d) inhibition of fretting through the development of a protective continuous surface oxide film.

2. At low temperature (room temperature) the role of oxidation in the fretting wear process is primarily an interactive rather than a controlling role. The interaction appears to be with surface fatigue mechanisms, and is generally strong.

3. With increased temperature, the kinetics of oxidation and the structure, composition, and properties of the oxide film play an increasingly important and ultimately controlling role in the fretting process.

4. For a given metal or alloy; for which oxidation behavior is generally well known, a predictive fretting model may be developed provided the wear characteristics of the oxides are understood.

REFERENCES

1. Waterhouse, R. B., "Fretting in Hostile Environments," Wear, Vol. 34, 1975, pp. 301-309.

2. Hurricks, P. L., "The Fretting Wear of Mild Steel From Room Temperature to 200° C," Wear, Vol. 19, 1972, pp. 207-229.

3. Hurricks, P. L., "The Fretting Wear of Mild Steel from 200° to 500° C," Wear, Vol. 30, 1974, pp. 189-212.

4. Feng, I-M., and Uhlig, H. H., "Fretting Corrosion of Mild Steel in Air and in Nitrogen," Journal of Applied Mechanics, Vol. 21, No. 4, Dec. 1954, pp. 395-400.

5. Bill, R. C., "Fretting of Nickel Chromium Aluminum Alloys at Temperatures to 816° C," NASA TN D-7570, 1974.

6. Bethune, B., and Waterhouse, R. B., "Adhesion of Metal Surfaces Under Fretting Conditions, I: Like Metals in Contact," Wear, Vol. 12, 1968, pp. 289-296.

7. Bill, R. C., "Study of Fretting Wear in Titanium, Monel-400, and Cobalt-25 Percent Molybdenum Using Scanning Electron Microscopy," American Society of Lubrication Engineers Transactions, Vol. 16, No. 4, 1973, pp. 286-290.

8. Waterhouse, R. B., Fretting Corrosion, Pergamon, New York, 1972, p. 124.

9. Kofstad, P., High-Temperature Oxidation of Metals, Wiley, New York, 1966, p. 274.

10. Hauffe, K., Oxidation of Metals, Plenum, New York, 1965, p. 179.

11. Giggins, C. S., and Pettit, F. S., "Oxidation of Ni-Cr-Al Alloys Between 1000° and 1200° C," Journal of the Electrochemical Society: Solid State Science, Vol. 118, No. 11, Nov. 1971, pp. 1782-1790.

12. Stott, F. H., Wood, G. C., and Hobby, M. G., "A Comparison of the Oxidation Behavior of Fe-Cr-Al, Ni-Cr-Al, and Co-Cr-Al Alloys," Oxidation of Metals, Vol. 3, No. 2, Mar. 1971, pp. 103-113.

13. Flower, H. M., and Swann, P. R., "An IN SITU Study of Titanium Oxidation by High-Voltage Electron Microscopy," Acta Metallurgica, Vol. 22, No. 11, Nov. 1974, pp. 1339-1347.

14. Kofstad, P., "High Temperature Oxidation of Metals," Wiley, New York, 1966, p. 46.

15. Bill, R. C., "Fretting Wear of Iron, Nickel, and Titanium Under Varied Environmental Conditions," NASA TM-78972, 1978.

16. Waterhouse, R. B., Fretting Corrosion, Pergamon, New York, 1972, p. 117.

17. Bill, R. C., "Fretting of Secondary-Sealking Candidate Materials in Air at Temperatures to 816° C," NASA TN D-7073, 1972.

18. Uhlig, H. H., "Mechanism of Fretting Corrosion," Journal of Applied Mechanics, Vol. 21, No. 4, Dec. 1954, pp. 401-407.

19. Weertmen, J., and Weertman, J. R., Elementary Dislocation Theory, Macmillan, New York, 1964, p. 189.

20. Quinn, T. F. J., "Oxidational Wear," Wear, Vol. 18, 1971, pp. 413-419.

21. Quinn, T. F. J., Sullivan, J. L., Rowson, D. M., "New Developments in the Oxidational Theory of the Mild Wear of Metals," Wear of Materials, K. C. Ludema, W. A. Glaeser, and S. K. Rhee, eds., American Society of Mechanical Engineers, New York, 1979, pp. 1-11.

22. Bill, R. C., "Fretting of Titanium at Temperatures to 650° C in Air," NASA TN D-8084, 1975.

TABLE I. - FRETTING MECHANISM SUMMARY

MATERIAL	CONDITIONS	BEHAVIOR TYPE
Ti	AIR, $<540^{0}$ C	III + II
	AIR, $>540^{0}$ C	IV
	NITROGEN	I + III (FATIGUE ONLY)
Ni-10 Cr-5 Al	AIR, $<650^{0}$ C	III + II
	AIR, $>650^{0}$ C	IV + III
Ni-10 Cr-2 Al	AIR, $<650^{0}$ C	III
	AIR, $>650^{0}$ C	III + QUINN OX. WEAR
Ni-20 Cr-5 Al	AIR, $<650^{0}$ C	III
	AIR, $>650^{0}$ C	III + QUINN OX. WEAR
Ni-20 Cr-2 Al	AIR, $<650^{0}$ C	III
	AIR, $>650^{0}$ C	III + QUINN OX. WEAR
TURBINE ALLOY VS. DAMPER COMB.	AIR, 23^{0} C ARGON, 23^{0} C	III I
	AIR, 816^{0} C ARGON, 816^{0} C	IV + III I + III (FATIGUE ONLY)

TYPE I: ADHESION + PLASTIC FLOW
TYPE II: OXIDE FILM REMOVAL WITH EACH FRETTING CYCLE
TYPE III: FATIGUE + OXIDATION
TYPE IV: OXIDE FILM REMAINS INTACT
QUINN OXIDATIVE WEAR: OXIDE FILM SPALLS AFTER REACHING CRITICAL THICKNESS

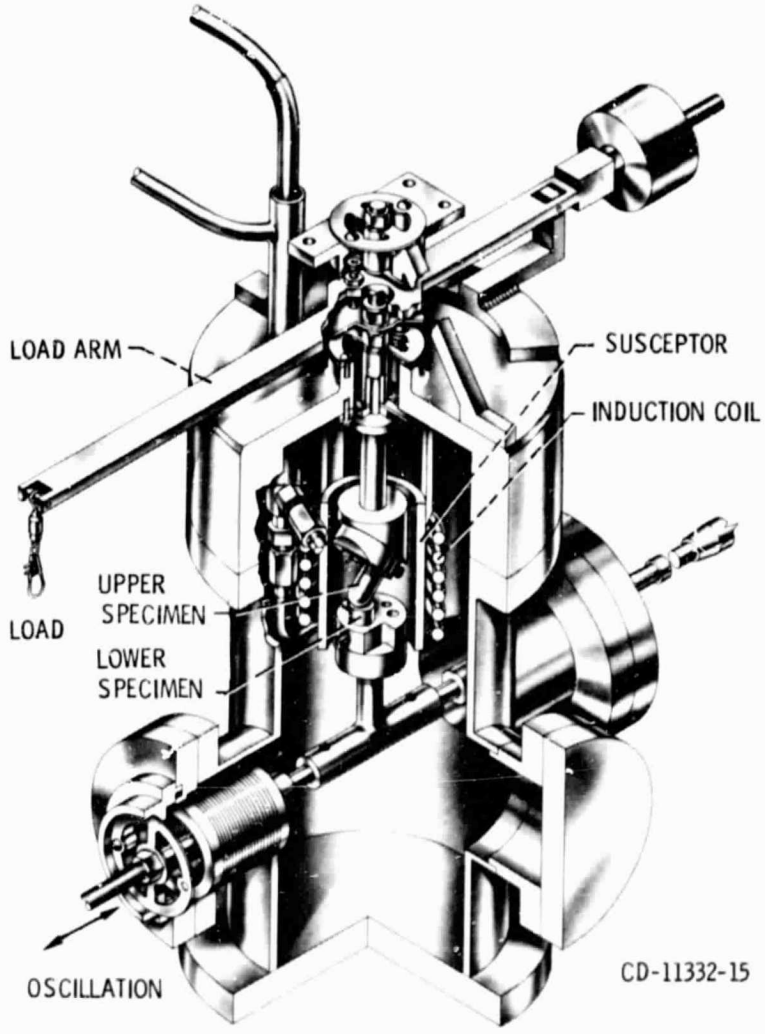

Figure 1. - Fretting apparatus.

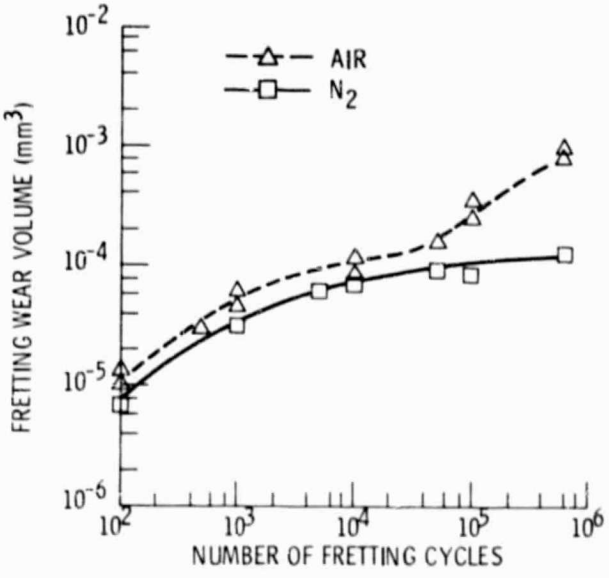

Figure 2. - Fretting wear volume versus number of fretting cycles for titanium in air and N_2. Fretting frequency, 55.8 Hz; amplitude, 75 μm; normal load, 1.47 N.

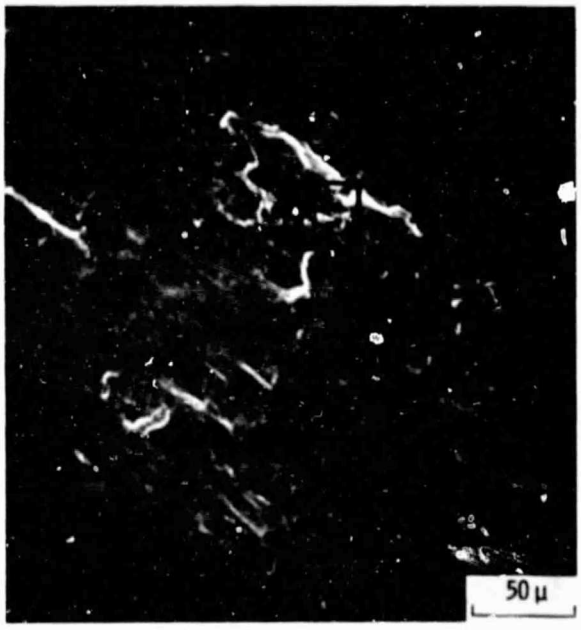

(a) 10^3 CYCLES, OVERVIEW.

(b) 10^3 CYCLES, AREA INDICATED IN BOX.

Figure 3. - Scanning electron micrographs of the fretted surfaces on titanium after the indicated number of fretting cycles in air at room temperature. Fretting frequency, 55.8 Hz; amplitude, 70 μm; normal load, 1.47 N.

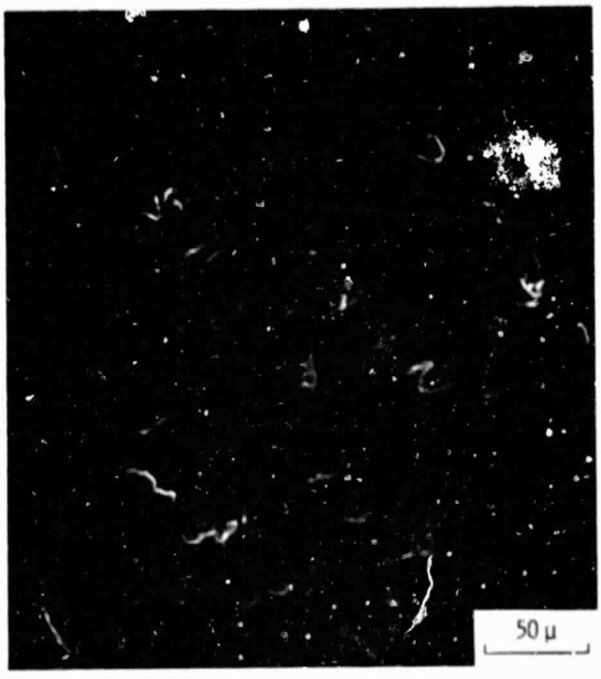

(c) 10^5 CYCLES, OVERVIEW.

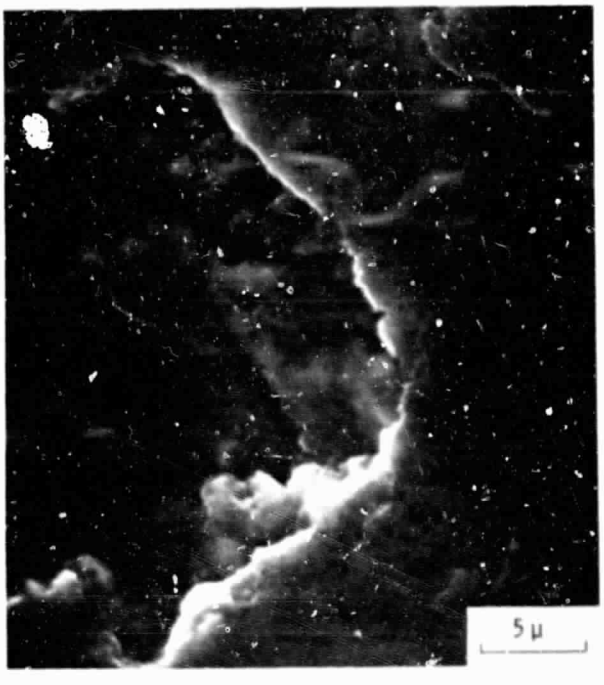

(d) 10^5 CYCLES, AREA INDICATED IN BOX.

Figure 3. - Concluded.

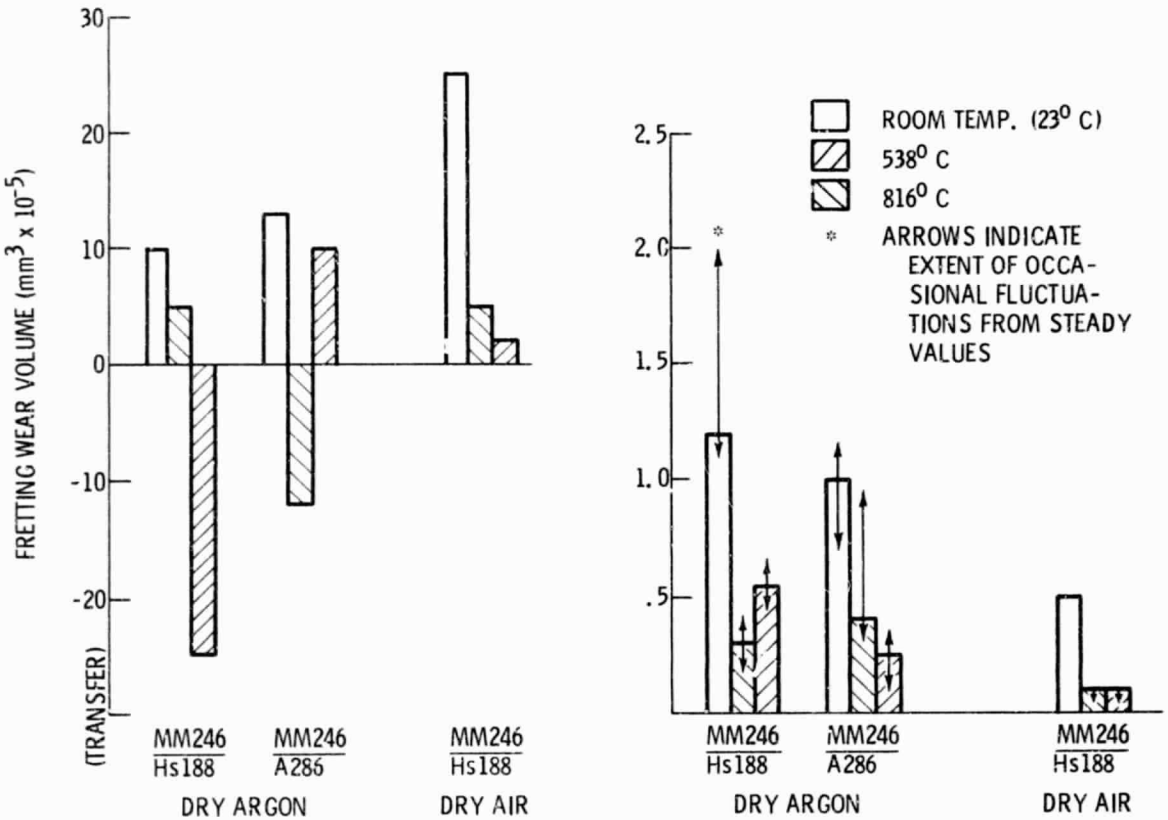

Figure 4. - Fretting wear volume to Mar M-246 (MM-246) and friction coefficient after fretting against Haynes 188 (Hs 188) and A-286 under the indicated conditions. Fretting frequency, 80 Hz (wear); 40 Hz (friction); amplitude, 40 μm; normal load, 1.47 N.

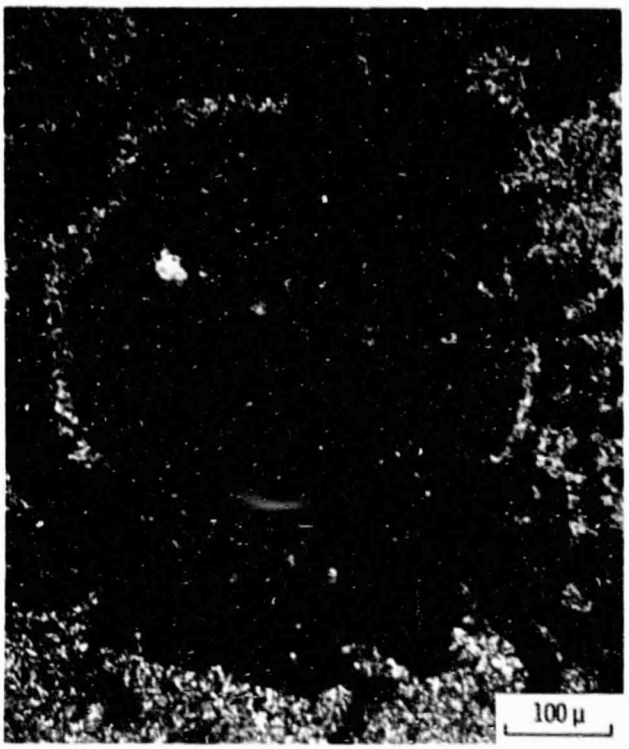

(a) DRY AIR.

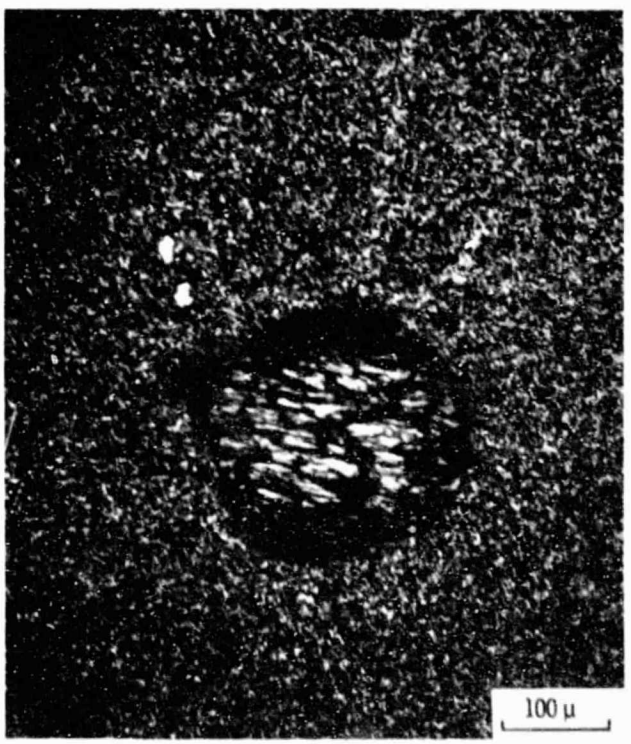

(b) DRY ARGON.

Figure 5. - Fretting wear scars on Mar M-246 after 3×10^5 cycles at room temperature in the indicated environment. Fretting frequency, 80 Hz; amplitude, 40 μm; normal load, 1.47 N.

(a) DRY ARGON.

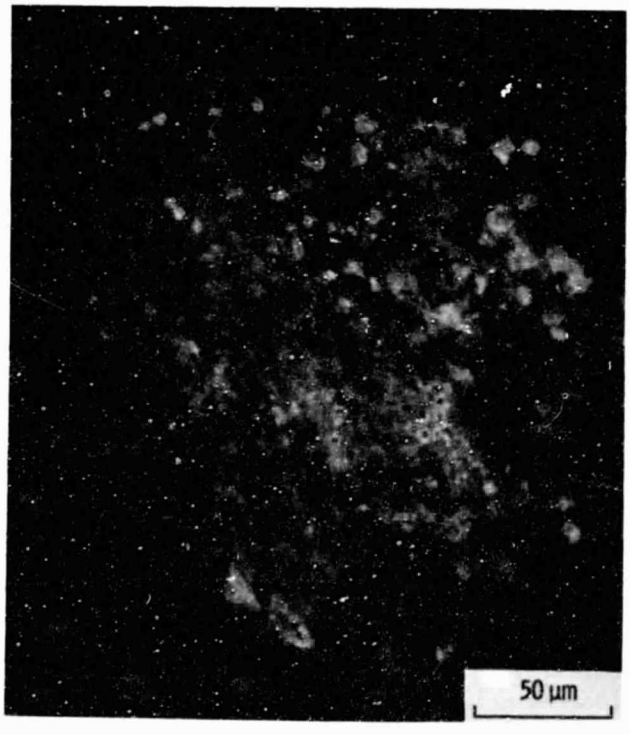

(b) DRY AIR.

Figure 6. - Fretting wear scars on Mar M-246 after 3×10^5 cycles against Haynes 188 at 816^0 C in the indicated environment. Fretting frequency, 80 Hz; amplitude, 40 µm; normal load, 1.47 N.

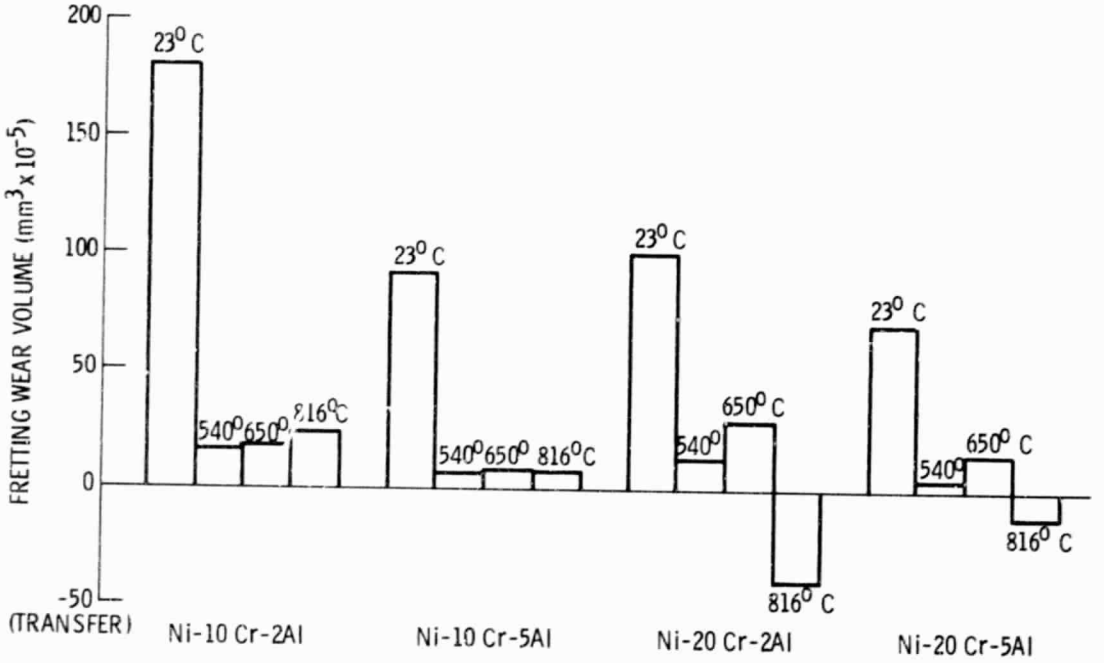

Figure 7. - Wear volume of Ni-Cr-Al alloys after 3×10^5 fretting cycles in dry air at the indicated temperatures. Fretting frequency, 80 Hz; amplitude, 70 μm; normal load, 1.47 N.

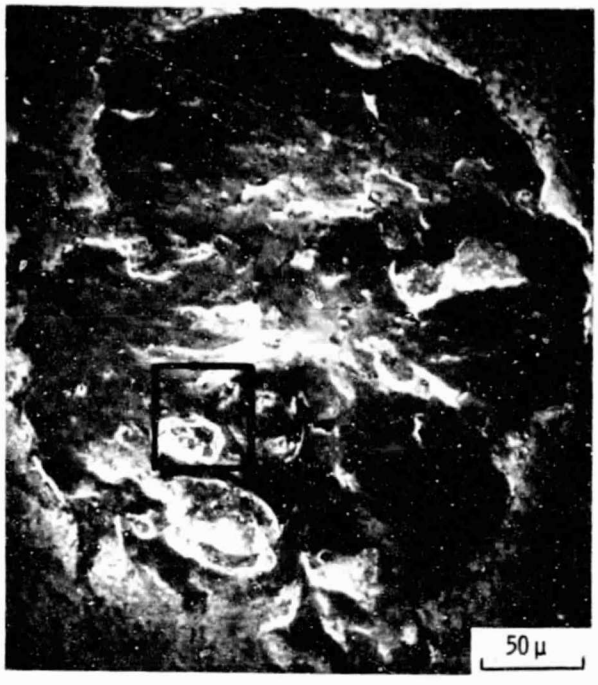

(a) OVERVIEW.

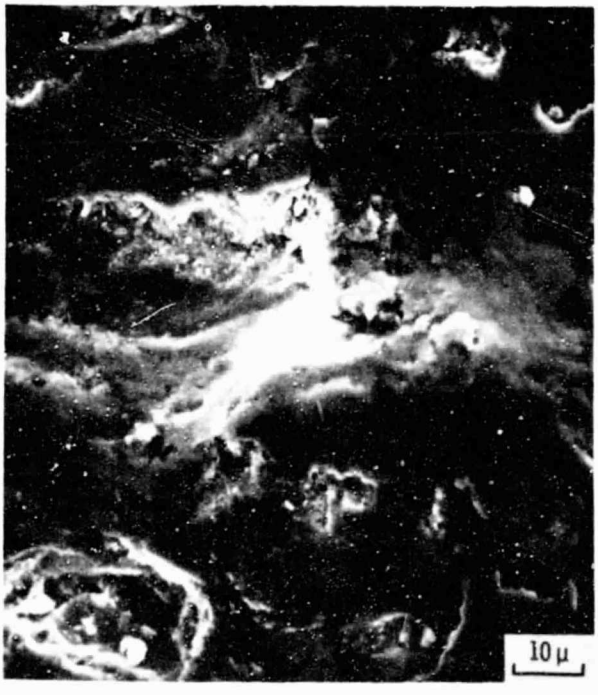

(b) AREA INDICATED IN BOX.

Figure 8. - Fretting wear scar on Ni-20Cr-2Al after 3×10^5 cycles at 816^0 C in air. Fretting frequency, 80 Hz; amplitude, 70 μm; normal load, 1.47.

(a) OVERVIEW.

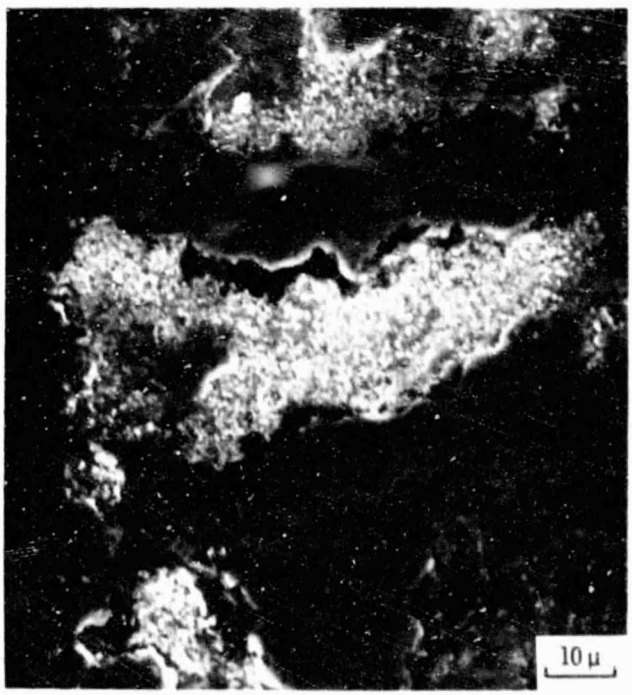

(b) AREA INDICATED IN BOX.

Figure 9. - Fretting wear scar on Ni-10Cr-2Al after $3x10^5$ cycles at 816^0 C in air. Fretting frequency, 80 Hz; amplitude, 70 um; normal load, 1.47 N.

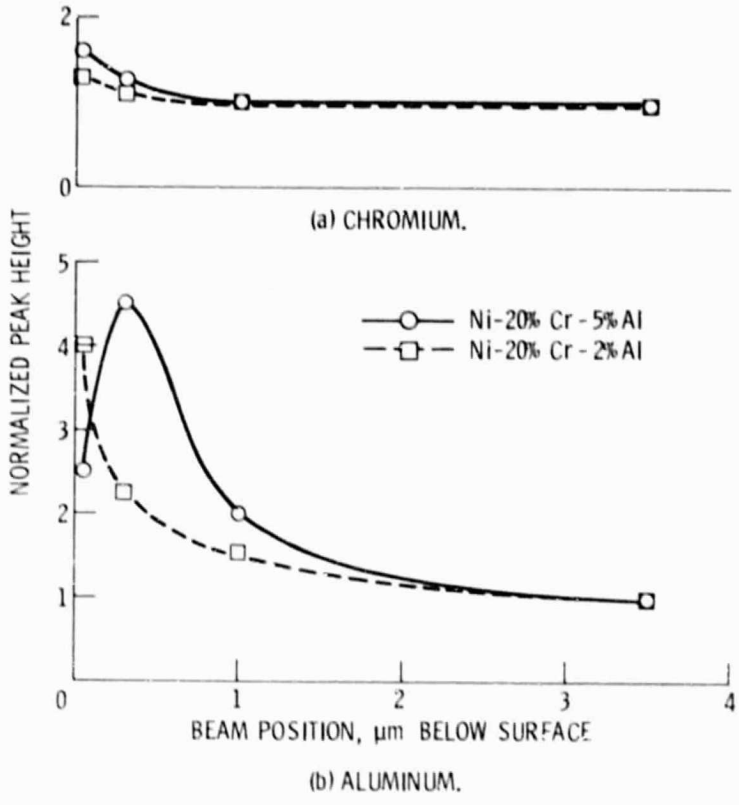

Figure 10. - Chromium and aluminum x-ray dispersion peak heights, normalized with respect to apparent bulk composition, as a function of electron beam position depth below surface.

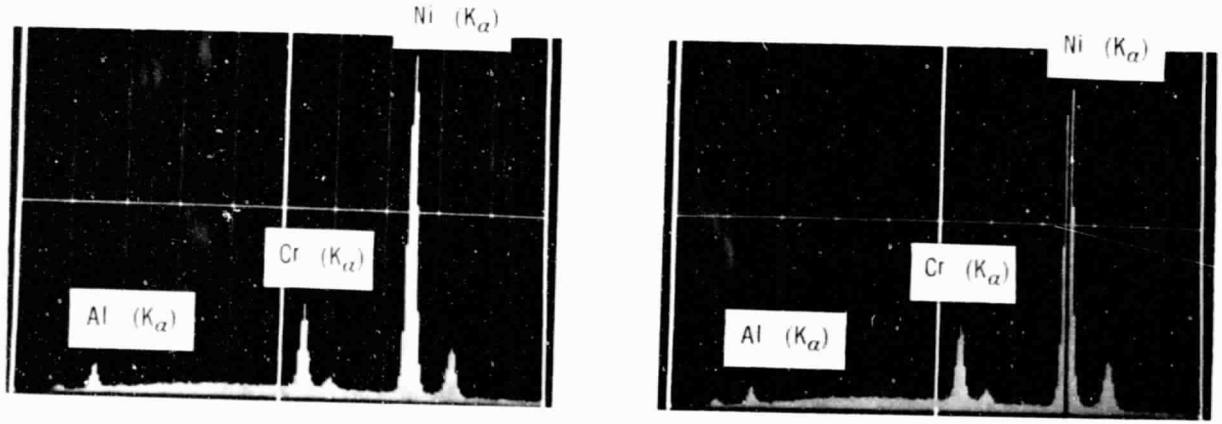

(a) Ni-10Cr-5Al.

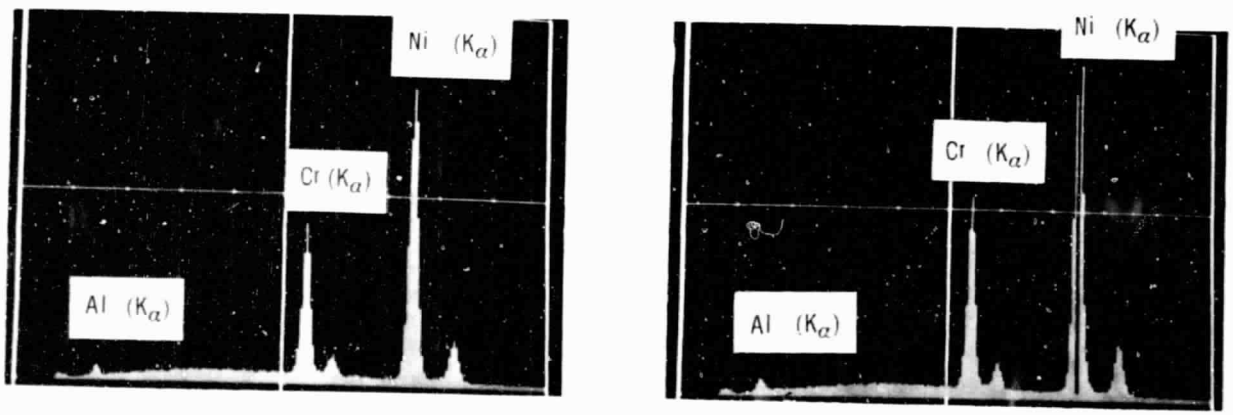

(b) Ni-20Cr-5Al.

Figure 11. - X-ray dispersion analyses of Ni-10Cr-5Al and Ni-20Cr-5Al within and outside the fretted area after fretting in dry air at 650° C.

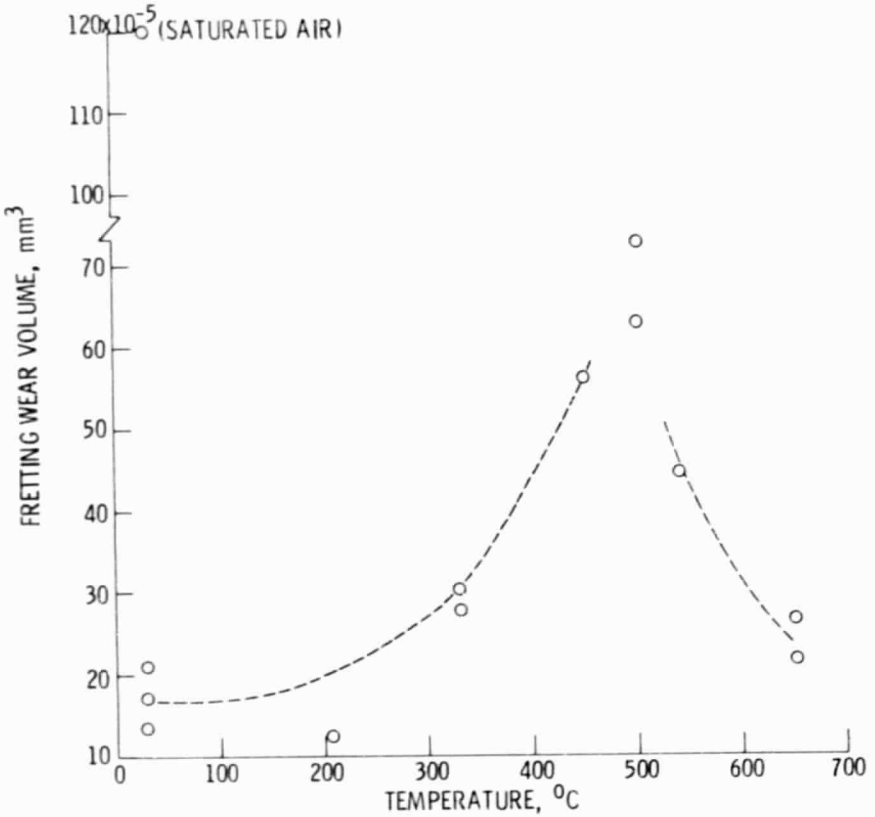

Figure 12. - Fretting wear volume plotted against temperature for high-purity titanium after $3x10^5$ fretting cycles under 1.47-newton normal load. Frequency, 80 hertz; dry air environment. Amplitude, 70 μm.

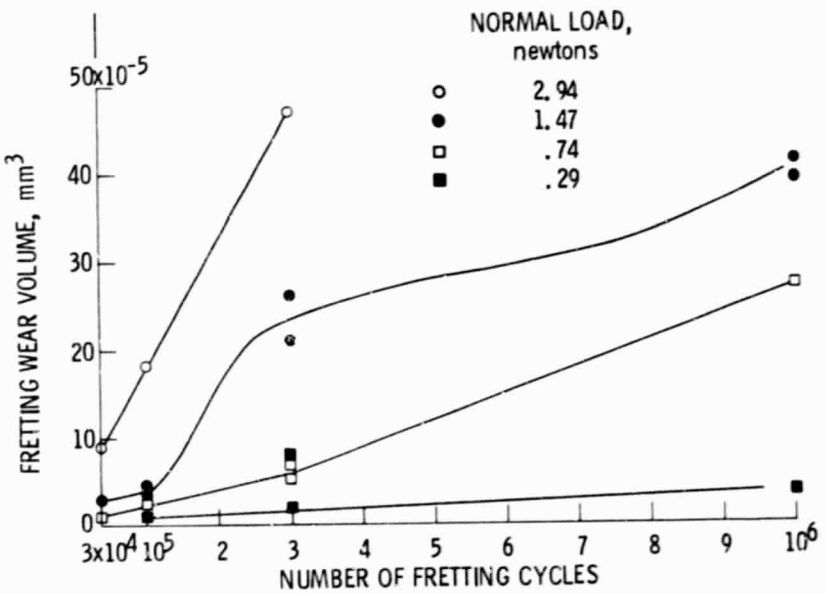

Figure 13. - Fretting wear plotted against number of fretting cycles for high-purity titanium at 650° C. Frequency, 80 hertz; dry air environment; amplitude, 70 micrometers.

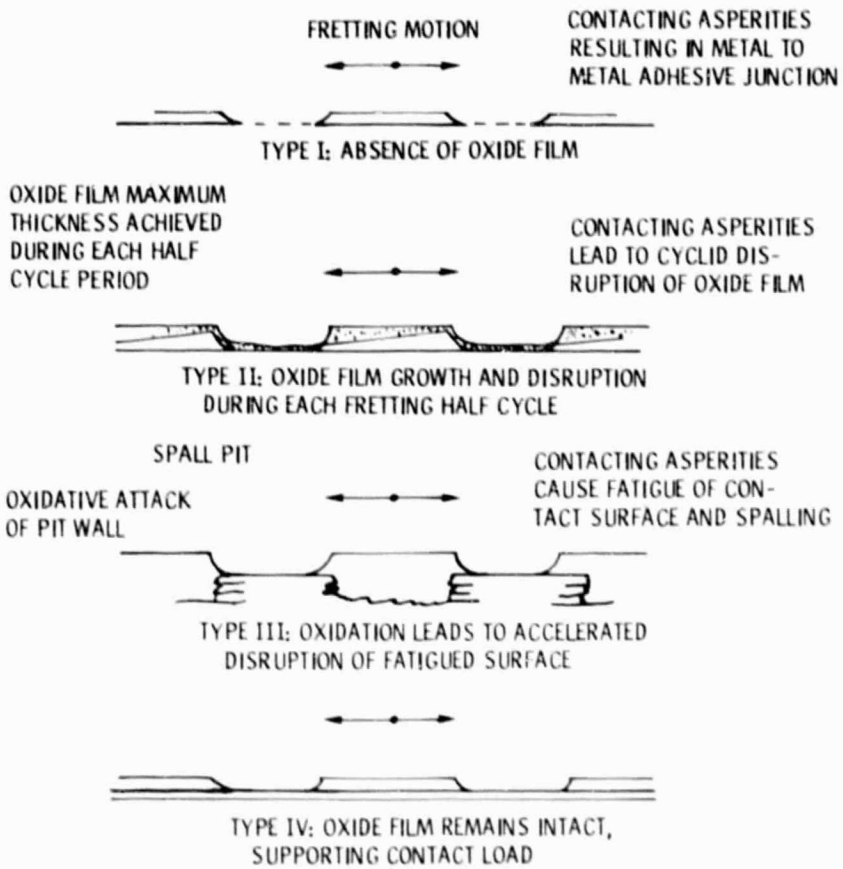

Figure 14. - Four types of interactions between fretting and oxidation.

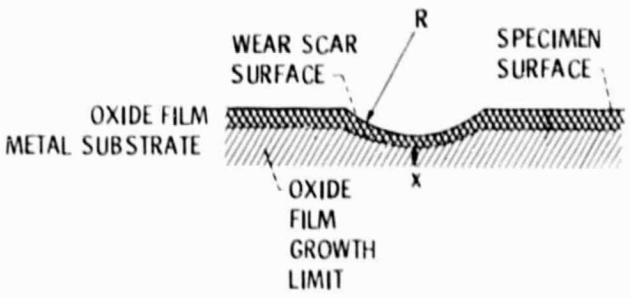

(a) FRETTING WEAR SCAR SECTION GEOMETRY.

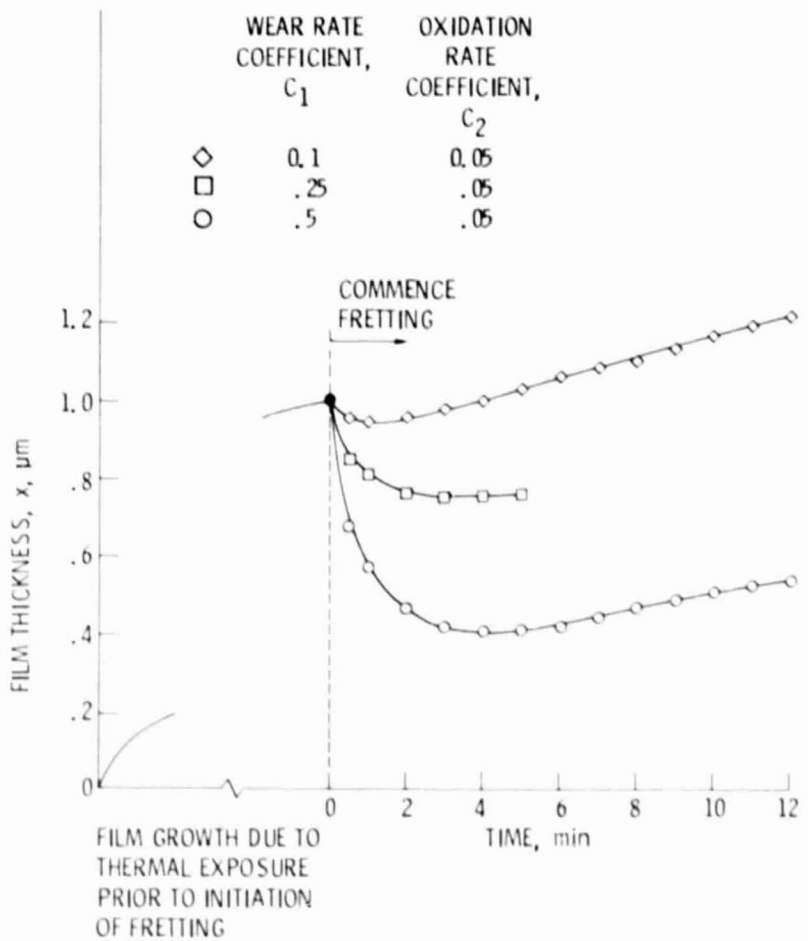

(b) PREDICTED OXIDE FILM THICKNESS UNDER FRETTING CONDITIONS AS FUNCTION OF TIME.

Figure 15. - Contact geometry and oxide film thickness for intact, parabolic film growth under sphere-on-flat fretting geometry conditions.